Effect of plasmodial RESA protein on deformability of human red blood cells harboring *Plasmodium falciparum*

J. P. Mills*, M. Diez-Silva*†, D. J. Quinn‡, M. Dao*, M. J. Lang§, K. S. W. Tan¶, C. T. Lim‖, G. Milon**, P. H. David†, O. Mercereau-Puijalon†, S. Bonnefoy†,††, and S. Suresh*‡§††

Departments of *Materials Science and Engineering and ‡Mechanical Engineering and §Division of Biological Engineering, Massachusetts Institute of Technology, Cambridge, MA 02139; †Unité d'Immunologie Moléculaire des Parasites, Centre National de la Recherche Scientifique, Unité de Recherche Associée 2581, Département de Parasitologie et Mycologie, Institut Pasteur, 75724 Paris, France; ¶Department of Microbiology, Yoo Loo Lin School of Medicine, National University of Singapore, Singapore 117597; ‖Division of Bioengineering and Department of Mechanical Engineering, Faculty of Engineering, National University of Singapore, Singapore 117576; and **Unité d'Immunophysiologie et Parasitisme Intracellulaire, Département de Parasitologie et Mycologie, Institut Pasteur, 75724 Paris, France

Communicated by Zdeněk P. Bažant, Northwestern University, Evanston, IL, April 13, 2007 (received for review February 4, 2007)

During intraerythrocytic development, *Plasmodium falciparum* exports proteins that interact with the host cell plasma membrane and subplasma membrane-associated spectrin network. Parasite-exported proteins modify mechanical properties of host RBCs, resulting in altered cell circulation. In this work, optical tweezers experiments of cell mechanical properties at normal physiological and febrile temperatures are coupled, for the first time, with targeted gene disruption techniques to measure the effect of a single parasite-exported protein on host RBC deformability. We investigate *Pf*155/Ring-infected erythrocyte surface antigen (RESA), a parasite protein transported to the host spectrin network, on deformability of ring-stage parasite-harboring human RBCs. Using a set of parental, gene-disrupted, and revertant isogenic clones, we found that RESA plays a major role in reducing deformability of host cells at the early ring stage of parasite development, but not at more advanced stage. We also show that the effect of RESA on deformability is more pronounced at febrile temperature, which ring-stage parasite-harboring RBCs can be exposed to during a malaria attack, than at normal body temperature.

malaria | erythrocyte | membrane shear modulus | spectrin | cytoskeleton

After *Plasmodium falciparum* merozoite invasion of a human RBC, the parasite differentiates and multiplies for 48 h, leading to rupture of the parasitized RBC (*Pf*-RBCs) and release of new merozoites in the blood circulation. Throughout this 48-h period, several parasite proteins are introduced into the RBC plasma membrane and submembranous protein skeleton, thereby modifying a range of structural and functional properties of the *Pf*-RBCs (1–4). The best documented changes occur as *P. falciparum* matures to the trophozoite (24–36 h) and schizont (36–48 h) stages, when *Pf*-RBCs display decreased membrane deformability (2–6), become spherical, and develop cytoadherence properties responsible for parasite sequestration in the postcapillary venules of different organs (7, 8). In contrast, during early parasite development, ring-stage (0–24 h after invasion) *Pf*-RBCs preserve their biconcave shape, can circulate in peripheral blood (9), and thus are exposed to the spleen red pulp. Ring-stage *Pf*-RBCs may pass through this spleen compartment, be expelled from circulation, or return to the circulation once the parasite has been removed (10). Although the relative importance of these different processes and their underlying mechanisms are not fully understood, it is likely that altered deformability of ring-stage *Pf*-RBCs (11) plays a crucial role in determining *Pf*-RBCs spleen processing.

Introduction of parasite components within the *Pf*-RBC membrane and cortical cytoskeleton begins soon after RBC invasion, as demonstrated for the well characterized parasite protein *Pf*155/Ring-infected erythrocyte surface antigen (RESA) (12). This protein is discharged by the invading merozoite and exported to the *Pf*-RBC membrane where, once phosphorylated, it interacts with the spectrin network (13). Because spectrin plays a critical role in the ability of RBCs to deform (14, 15), it has been proposed that RESA could play an important role in the modulation of mechanical properties of ring-stage *Pf*-RBCs (1, 6). A connection between RESA and altered *Pf*-RBC mechanical properties has been demonstrated in a previous study on *Pf*-RBC membrane stability. *Pf*-RBCs *resa1* knockout (KO) parasites obtained by gene disruption were prone to heat-induced vesiculation when exposed at 50°C, whereas *resa1*+ *Pf*-RBCs were not (16). This observation confirmed previous conclusions about the stabilization effect of RESA on the RBC submembranous cytoskeleton against heat-induced structural changes (17). However, analysis of RBC membrane deformability using a micropipette approach did not show any significant modification of membrane mechanical properties (16).

Here we demonstrate a new biophysical experimental technique for measuring the effect of a single parasite-exported protein, in this case RESA, on the overall deformability of pathologic RBCs harboring *P. falciparum*. Previously, optical tweezers were used to characterize mechanical property changes induced by *P. falciparum* over all intraerythrocytic developmental stages (4, 18). To study the effect of ultrastructural changes induced by parasite-exported proteins on parasitized RBC deformability, we coupled optical tweezers experiments with targeted gene disruption, a cell biology technique to prevent production of a specific protein. Through a combination of these methods adapted from different fields, we assessed, to a force resolution of a pN, the question of the role of RESA on RBC deformability. To ascertain the role of RESA, we constructed a set of three isogenic cloned parasite lines, a *resa1* wild type, a *resa1*-KO targeted gene disruptant clone, and the *resa1*+ revertant of this clone. Tests were conducted at room temperature to comply with standard deformability assays, as well as at 37°C and 41°C to investigate possible effects on deformability resulting from febrile temperature to which ring-stage *Pf*-RBCs are exposed during a malaria attack.

Author contributions: J.P.M. and M.D.-S. contributed equally to this work; J.P.M., M.D.-S., G.M., P.H.D., O.M.-P., S.B., and S.S. designed research; J.P.M., M.D.-S., and D.J.Q. performed research; M.D., M.J.L., K.S.W.T., C.T.L., S.B., and S.S. contributed new reagents/analytic tools; J.P.M. and M.D. analyzed data; and J.P.M., M.D.-S., M.D., G.M., P.H.D., O.M.-P., S.B., and S.S. wrote the paper.

The authors declare no conflict of interest.

Freely available online through the PNAS open access option.

Abbreviations: RESA, Ring-infected erythrocyte surface antigen; KO, knockout.

††To whom correspondence may be addressed. E-mail: sbf@pasteur.fr or ssuresh@mit.edu.

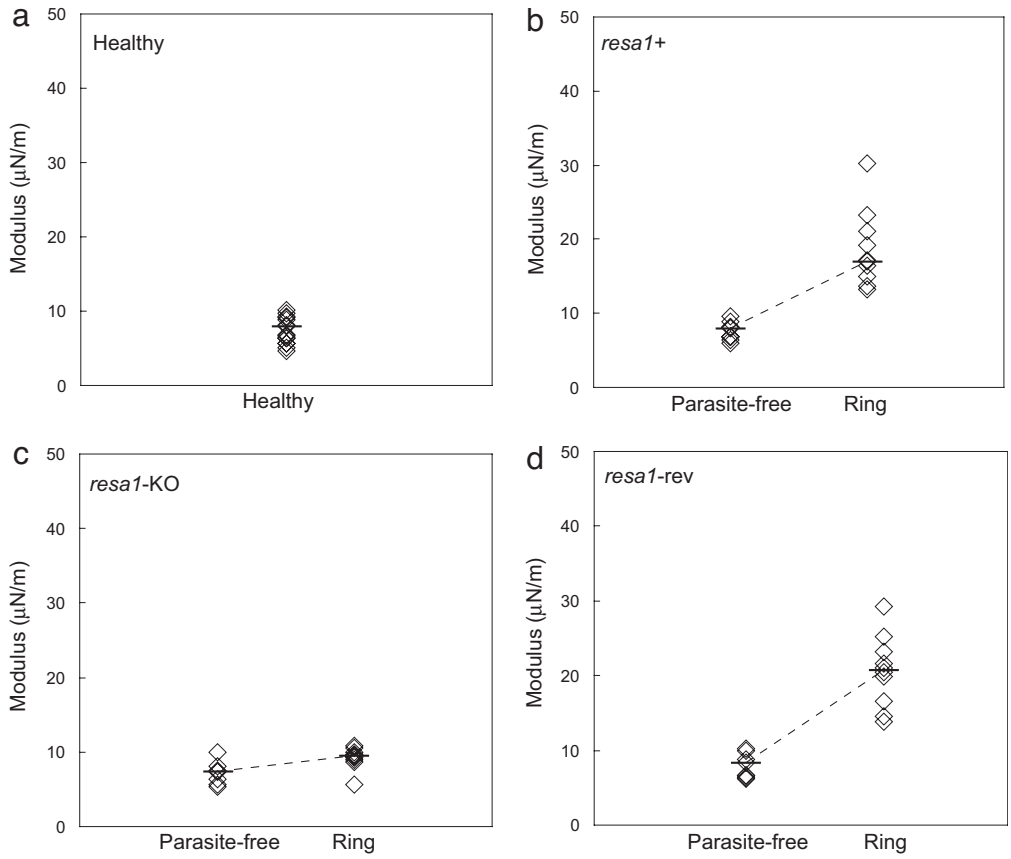

Fig. 1. Stiffness of healthy, parasite-free, and late ring-stage (14–20 h after invasion) *Pf*-RBCs at room temperature (25°C). Tests were performed on cultures of healthy RBCs (*a*), wild-type *resa1*+ *Pf*-RBCs (*b*), *resa1*-KO *Pf*-RBCs (*c*), and *resa1-rev Pf*-RBCs (*d*).

RBC deformability is significantly dependent on RBC membrane stiffness. Our optical tweezers experiments led to a quantitative measure of membrane stiffness by determining the shear modulus, μ, of the RBC membrane. An increase in membrane stiffness corresponds to an overall decrease in RBC deformability.

Results

Effect of RESA Protein on Ring-Stage *Pf*-RBC Deformability. Measurement of RBC membrane stiffness (hereafter referred to as stiffness) for *Pf*-RBCs was performed on late ring-stage *Pf*-RBCs (14–20 h after invasion) harboring wild-type *resa1*+, *resa1*-KO, and *resa1-rev* parasites. The *resa1*-KO parasites were generated by insertion into the *resa1* locus on chromosome 1 of a plasmid containing a positive and a negative selection marker. The *resa1-rev* were derived from the *resa1*-KO clone by negative selection using ganciclovir (see *Materials and Methods*). Control tests were performed on healthy RBCs maintained under standard *Pf*-RBC culture conditions and parasite-free RBCs. (Parasite-free RBCs were present in *Pf*-RBC cultures but did not harbor any parasites.) Tests were first performed at room temperature (25°C) (Fig. 1).

Consistent with earlier work based on micropipette aspiration (19) and optical tweezers (20), the measured stiffness of healthy RBCs was 5–10 μN/m (median μ = 6.8 μN/m) (Fig. 1*a*). The stiffness of late ring-stage *resa1*+ *Pf*-RBCs (μ = 17.7 μN/m) (Fig. 1*b*) increased significantly compared with healthy RBCs ($P < 0.0001$). The 2-fold increase in membrane shear modulus for *resa1*+ *Pf*-RBCs is consistent with previous work using 3D7, a *resa1*+ *P. falciparum* clone (4, 11).

In contrast, late ring-stage *resa1*-KO *Pf*-RBCs (μ = 9.4 μN/m) (Fig. 1*c*) displayed a stiffness similar to healthy RBCs. The observed stiffness of *resa1*-KO *Pf*-RBCs was significantly different compared with wild-type *resa1*+ *Pf*-RBCs ($P < 0.0001$).

To ensure that targeted gene disruption of *resa1* (and hence the absence of RESA) was responsible for the results observed in *resa1*-KO *Pf*-RBCs, we tested *resa1-rev Pf*-RBCs (Fig. 1*d*). The measured stiffness of *resa1-rev Pf*-RBCs (μ = 20.8 μN/m) was similar to that of the *resa1*+ *Pf*-RBCs, with a significantly higher shear modulus compared with healthy RBCs ($P < 0.0001$) and *resa1*-KO *Pf*-RBCs ($P < 0.001$).

Parasite-free RBCs from wild-type *resa1*+, *resa1*-KO, and *resa1-rev* parasite cultures (Fig. 1 *b–d*, respectively) displayed similar stiffness compared with healthy RBCs (Fig. 1*a*).

Effect of RESA Protein on Trophozoite-Stage *Pf*-RBC Deformability. To determine whether the presence of RESA protein at the ring stage is needed for implementing the changes of the mechanical properties displayed by subsequent mature stages of *Pf*-RBCs, we measured the stiffness of *resa1*+ and *resa1*-KO trophozoite-stage *Pf*-RBCs (24–36 h after invasion). The stiffness of trophozoite-stage *resa1*+ (μ = 35.9 μN/m) and *resa1*-KO (μ = 35.7 μN/m) *Pf*-RBCs (Fig. 2) was significantly higher than ring-stage *resa1*+ *Pf*-RBCs ($P < 0.001$) and *resa1*-KO ($P < 0.001$), respectively. The 4-fold increase in shear modulus measured for both *resa1*+ and *resa1*-KO trophozoite-stage *Pf*-RBCs is consistent with previous studies (4, 11). No difference in stiffness between *resa1*+ and *resa1*-KO *Pf*-RBCs was observed at the trophozoite stage.

Impact of Physiological (Steady-State and Febrile) Temperatures on Ring-Stage *Pf*-RBC Deformability. To study *Pf*-RBC deformation at physiological temperature and the consequences of elevated

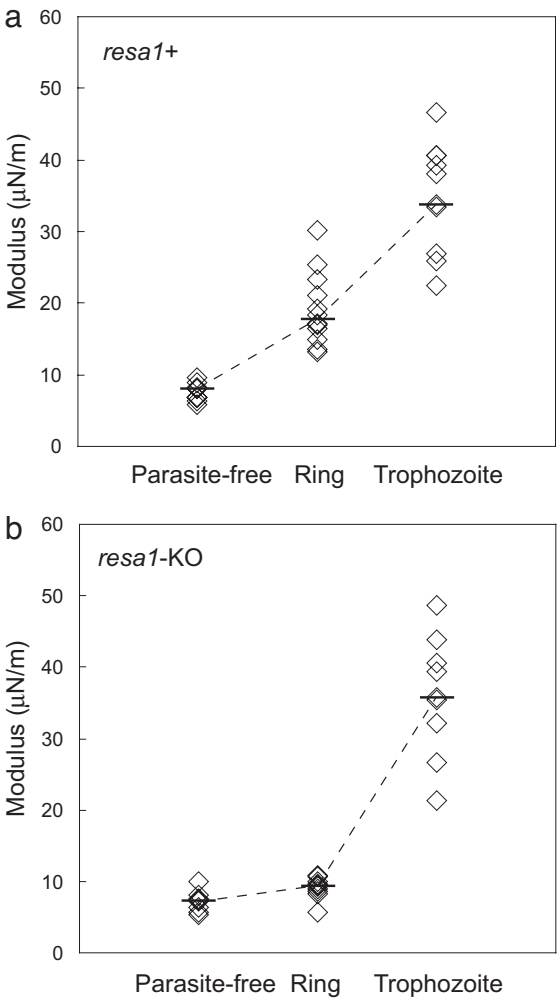

Fig. 2. Stiffness over progressive parasite maturation from the ring stage (12–24 h after invasion) to the trophozoite stage (24–36 h after invasion) at room temperature (25°C). Tests were performed on cultures of wild-type *resa1*+ *Pf*-RBCs (*a*) and *resa1*-KO *Pf*-RBCs (*b*).

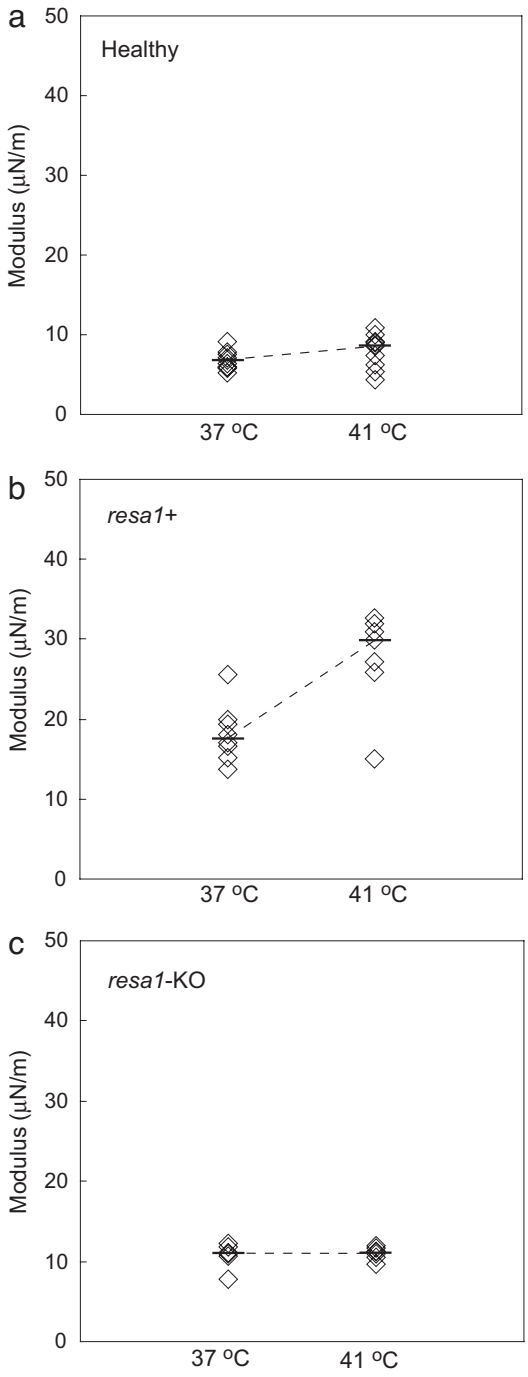

Fig. 3. Stiffness of RBCs and *Pf*-RBCs at normal body (37°C) and febrile (41°C) temperatures. Tests were performed on cultures of healthy RBCs (*a*), wild-type *resa1*+ *Pf*-RBCs (*b*), and *resa1*-KO *Pf*-RBCs (*c*).

body temperature during febrile malaria episodes, tests on *resa1*+ and *resa1*-KO ring-stage *Pf*-RBCs were carried out at normal body temperature (37°C) and febrile temperature (41°C) (Fig. 3*a*).

The stiffness of healthy RBCs at 37°C (μ = 6.6 μN/m) and 41°C (μ = 8.6 μN/m) was similar to healthy RBCs at room temperature (5–10 μN/m) (Fig. 1*a*). The observation that stiffness of healthy RBCs remains approximately constant over this temperature range is consistent with similar measurements using other techniques (19, 21).

Ring-stage *resa1*+ *Pf*-RBCs displayed a marked increase in stiffness both at 37°C (μ = 17.6 μN/m) and 41°C (μ = 29.9 μN/m) (Fig. 3*b*) compared with healthy RBCs. The stiffness increase for *resa1*+ *Pf*-RBCs was significantly greater at 41°C than at 37°C ($P < 0.05$). In contrast, the stiffness of *resa1*-KO *Pf*-RBCs (Fig. 3*c*) at 37°C (μ = 11 μN/m) and 41°C (μ = 11.2 μN/m) remained similar to measurements at room temperature (μ = 9.4 μN/m) (Fig. 1*c*).

Discussion

During intraerythrocytic development of *P. falciparum*, parasite-exported proteins contribute to modifications of the deformability of *Pf*-RBCs. The contribution of specific parasite-exported proteins to decreased deformability has been demonstrated for KAHRP and PfEMP3 (5), which are present in the erythrocyte membrane in the trophozoite and schizont stages when *Pf*-RBCs are sequestered. Our study explores the effect of RESA, a ring-stage parasite-exported protein, on altered deformability of *Pf*-RBCs that are not sequestered and, therefore, must circulate. We document here a significantly reduced deformability by measuring the stiffness of ring-stage *Pf*-RBCs, and we show that RESA is largely responsible for this mechanical property change.

Whereas measured healthy RBC stiffness remained constant over all test temperatures, increased stiffness of ring-stage

Pf-RBCs was greater at febrile temperature than at normal body temperature. Because *resa1*-KO *Pf*-RBCs exhibited stiffness similar to healthy RBCs at all temperatures, we conclude that the temperature-related change in membrane deformability is attributable, at least in part, to the presence of RESA in the ring-stage *Pf*-RBC membrane.

At the more advanced trophozoite stage, increased stiffness of *Pf*-RBCs was independent of a parasite's ability to express RESA. It has been shown that RESA can no longer be detected at the trophozoite stage (22), where parasite proteins other than RESA play a predominant role in decreased deformability, among which are KAHRP and PfEMP3 (5). Furthermore, our results indicate that absence of RESA in the ring stage does not impair subsequent remodeling in the late parasite stages.

Altered deformability during the ring stage is most probably a consequence of the attachment of RESA to spectrin (23). Binding of RESA to β1R16 spectrin structural repeat close to the interaction region between α1 and β1 spectrins significantly increases the stability of spectrin tetramers (24). In healthy RBCs, the spectrin network exists in a dynamic state of spectrin tetramers dissociating transiently into dimers, and shear deformation shifts the equilibrium of tetramer formation toward the dissociated dimer state (25). Thus, RESA stabilization of tetramers could modify spectrin network dynamic properties, thereby impairing membrane deformability.

This model is consistent with a proposed role for RESA on temperature-dependent membrane stability. Increased membrane resistance to thermal shift-induced structural change has been related to the stabilization of spectrin tetramers induced by RESA binding (24). Although the effect of temperature on the interaction between RESA and spectrin is unknown, we speculate that this specific binding alters temperature-dependent stabilization of spectrin tetramers and, as a consequence, contributes to the observed changes in ring-stage *Pf*-RBC deformability at febrile temperatures.

Deformability is critical for *in vivo* parasite survival during the ring stage when *Pf*-RBCs have not yet cytoadhered/sequestered and circulate in postcapillary microvessels and through the spleen. We have shown that ring-stage *Pf*-RBC decreased deformability is mediated/modulated by RESA, which binds to the RBC cytoskeleton. We find that the effect of RESA on deformability is greater at febrile temperature. It has been shown previously that exposure of ring-stage *Pf*-RBCs to febrile temperature negatively impacts parasite growth in the absence of RESA (16). RESA may thus play a role in the delicate balance between parasite and its host during the ring stage, on the one hand through contributing to parasite resistance to febrile temperatures and on the other hand through membrane deformability changes that may affect spleen processing of the *Pf*-RBC.

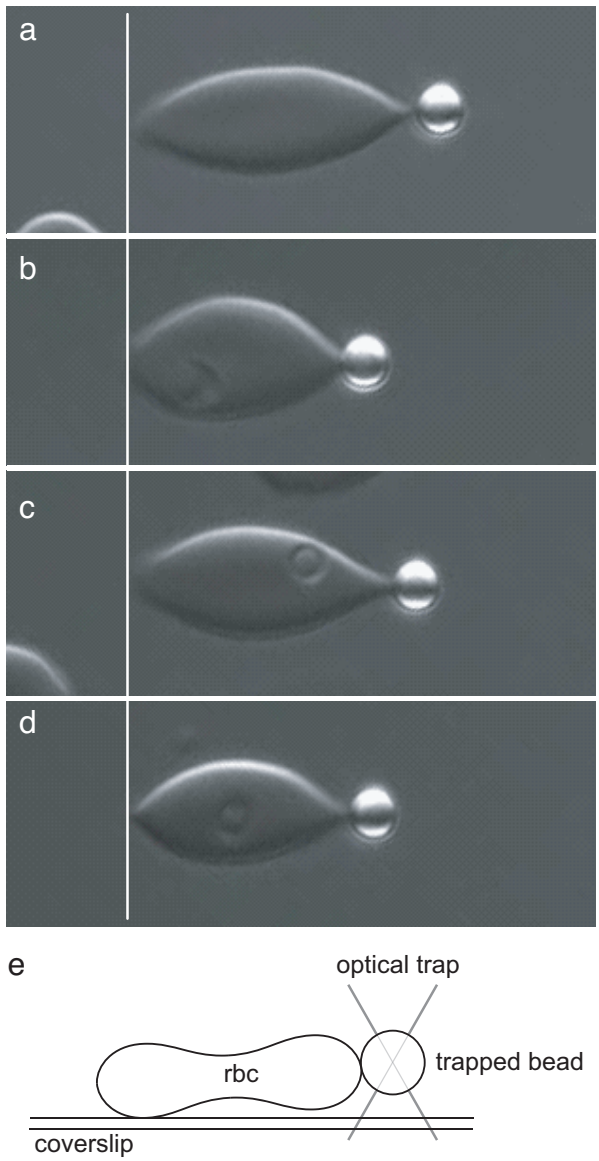

Fig. 4. Optical microscopy images of RBCs stretched by using optical tweezers. (*a–d*) Representative RBCs stretched uniaxially with a 100-pN force. The *resa1*-KO *Pf*-RBC (*c*) shows deformability similar to parasite-free RBCs (*a*), whereas wild-type *resa1*+ (*b*) and *resa1-rev Pf*-RBCs (*d*) display similar decreased deformability. Stiffness values are determined from the entire force versus displacement response of each cell. (e) A schematic representation of a side view of an optical tweezers stretch test where a RBC is stretched by holding it at the coverslip surface and at the trapped bead.

Materials and Methods

Plasmid Constructs and Gene Disruption. PCR-amplified full-length *P. falciparum resa1* gene was cloned in between SacII/XbaI sites of a modified pdTg23 vector (26) carrying the *Toxoplasma gondii* dihydrofolate reductase/thymidine synthase gene *dhfr/ts* (conferring resistance to pyrimethamine) fused in frame with the herpes virus thymidine kinase 1 (27, 28). Ring-stage FUP/CB (*resa1*+) clone parasites (FCR3-*resa1*+-like genotype) were transfected with 100 μg of Qiagen-purified targeting plasmid using the electroporation conditions described in ref. 29. Homologous recombination in the endogenous *resa1* gene was obtained after a two-step pyrimethamine pressure selection (26). Pyrimethamine-resistant parasites were cloned by limiting dilution. Ganciclovir (10 μM) drug pressure was applied on genetically confirmed *resa1*-KO parasites in the absence of pyrimethamine to induce the *resa1* gene reversion (*resa1-rev* parasites) (28).

Parasite Culture. A clone derived from *P. falciparum* (FUP/CB) parasites, named here wild-type *resa1*+ *P. falciparum*, was maintained in leukocyte-free human O+ erythrocytes (Research Blood Components, Brighton, MA) and stored at 4°C for no longer than 2 weeks under an atmosphere of 3% O_2, 5% CO_2, and 92% N_2 in RPMI medium 1640 (Gibco Life Technologies, Rockville, MD) supplemented with 25 mM Hepes (Sigma, St. Louis, MO), 200 mM hypoxanthine (Sigma), 0.209% $NaHCO_3$ (Sigma), and 0.25% albumax I (Gibco Life Technologies). Cultures were synchronized successively by concentration of mature schizonts using plasmagel flotation (30) and sorbitol lysis 2 h after the merozoite invasion to remove residual schizonts (31). For wild-type *resa1*+, *resa1*-KO, and *resa1-rev Pf*-RBCs tests, optical tweezers tests were performed within and 14–20 h

(ring stage) or 24–36 h (trophozoite stage) after merozoite invasion.

Bead Preparation. Two-micrometer-diameter, streptavidin-coated polystyrene beads (Polysciences, Warrington, PA) were centrifuged three times at 16,000 × *g* in 0.1 mg/ml BSA-PBS. The beads were incubated for 30 min at 4°C in 1 mg/ml Con A (Sigma). The beads were then centrifuged three more times at 16,000 × *g* in 0.1 mg/ml BSA-PBS and stored in 0.1 mg/ml BSA-PBS.

Sample Preparation. RBCs and *Pf*-RBCs were centrifuged at 125 × *g* three times in RPMI medium 1640 before suspension in 0.1 mg/ml BSA-PBS. Con A-coated polystyrene beads were added to the RBC suspension.

RBC Membrane Stiffness Measurement. An optical tweezers technique was used to measure single RBC force-displacement response, from which shear modulus values can be determined based on computational modeling (32, 33). Uniaxial tension tests on single RBCs required attaching a small portion of an RBC to the coverslip and, on the diametrically opposite side, to an optically trapped Con A-coated polystyrene bead (Fig. 4*e*). Movement of the coverslip via a piezo-stage (Physik Instrumente) applied deformations to the RBC with resolution <1 nm. Applied forces up to 300 pN, with resolution <5 pN, were continuously measured by detecting the position of the optically trapped bead with a laser-based position detection system. A standard optical tweezers calibration of trapping force exerted on a bead was performed before tests by subjecting the trapped bead to known forces via fluid flow (Stokes flow technique). During a stretch experiment, deformations and forces were continuously acquired to determine the force-displacement response of a single RBC. Shear modulus values were computed immediately after each experiment by fitting the experimental data to an analytical expression derived from computational modeling using a finite element method (33). This method using continuous acquisition of optical tweezers test data and concurrent data analysis based on finite element modeling provides a substantial improvement to existing techniques for single RBC mechanical property evaluation with optical tweezers (18, 20, 34).

Temperatures of 37°C and 41°C were achieved by locally heating the test sample with resistive heaters. Optical tweezers tests were conducted at these temperatures after maintaining the test temperature for 10 min. Two resistive heating pads attached to thin copper blocks were kept in thermal contact with the microslide to control the temperature at the sample. A thermocouple placed within the sample chamber was used to measure the local temperature, which was kept to ± 1°C.

Statistical Analysis. Reported shear modulus values in the text are median values from multiple measurements shown in the figures. *P* values are calculated by two-tailed Mann–Whitney rank sum tests comparing shear modulus values between various test conditions.

This work was supported by an interinstitution research grant made available through the National University of Singapore as part of the Global Enterprise for MicroMechanics and Molecular Medicine, Pasteur Transversal Research Program Grant PTR#59 (to S.B.), and a research grant from the Agence Nationale de Recherches sur le SIDA (to G.M.). S.S. further acknowledges support from the Computational Systems Biology Program of the Singapore–MIT Alliance.

1. Cooke BM, Mohandas N, Coppel RL (2001) *Adv Parasitol* 50:1–86.
2. Cranston HA, Boylan CW, Carroll GL, Sutera SP, Williamson JR, Gluzman IY, Krogstad DJ (1984) *Science* 223:400–403.
3. Paulitschke M, Nash GB (1993) *J Lab Clin Med* 122:581–589.
4. Suresh S, Spatz J, Mills JP, Micoulet A, Dao M, Lim CT, Beil M, Seufferlein T (2005) *Acta Biomater* 1:15–30.
5. Glenister FK, Coppel RL, Cowman AF, Mohandas N, Cooke BM (2002) *Blood* 99:1060–1063.
6. Nash GB, O'Brien E, Gordon-Smith EC, Dormandy JA (1989) *Blood* 74:855–861.
7. Dondorp AM, Pongponratn E, White NJ (2004) *Acta Trop* 89:309–317.
8. Miller LH, Baruch DI, Marsh K, Doumbo OK (2002) *Nature* 415:673–679.
9. Sherman IW, Eda S, Winograd E (2003) *Microbes Infect* 5:897–909.
10. Angus BJ, Chotivanich K, Udomsangpetch R, White NJ (1997) *Blood* 90:2037–2040.
11. Mills JP, Qie L, Dao M, Tan KSW, Lim CT, Suresh S (2005) *Mater Res Soc Symp Proc* 844:Y7.8.1–Y7.8.6.
12. Perlmann H, Berzins K, Wahlgren M, Carlsson J, Björkman A, Patarroyo ME, Perlmann P (1984) *J Exp Med* 159:1686–1704.
13. Foley M, Tilley L, Sawyer WH, Anders RF (1991) *Mol Biochem Parasitol* 46:137–147.
14. Bennet V, Lambert S (1991) *J Clin Invest* 87:1483–1489.
15. Mohandas N, Evans EA (1994) *Annu Rev Biophys Biomol Struct* 23:787–818.
16. Silva MD, Cooke BM, Guillotte M, Buckingham DW, Sauzet J-P, Scanf CL, Contamin H, David P, Mercereau-Puijalon O, Bonnefoy S (2005) *Mol Microbiol* 56:990–1003.
17. Da Silva E, Foley M, Dluzewski AR, Murray LJ, Anders RF, Tilley L (1994) *Mol Biochem Parasitol* 66:59–69.
18. Sleep J, Wilson D, Simmons R, Gratzer W (1999) *Biophys J* 77:3085–3095.
19. Waugh R, Evans EA (1979) *Biophys J* 26:115–131.
20. Mills JP, Qie L, Dao M, Lim CT, Suresh S (2004) *Mech Chem Biosyst* 1:169–180.
21. Li J, Huang YX, Ji T, Tu M, Mao X, Chen WX, Chen GW (2005) *Acta Biochim Biophys Sin* 37:391–395.
22. Coppel RL, Lustigman S, Murray L, Anders RF (1988) *Mol Biochem Parasitol* 31:223–231.
23. Foley M, Corcoran L, Tilley L, Anders R (1994) *Exp Parasitol* 79:340–350.
24. Pei X, Guo X, Coppel R, Haldar K, Gratzer W, Mohandas N, An X (2007) *Blood*, 10.1182/blood-2007-02-076919.
25. An X, Guo X, Zhang X, Baines AJ, Debnath G, Moyo D, Salomao M, Bhasin N, Johnson C, Discher D, *et al.* (2006) *J Biol Chem* 281:10527–10532.
26. Wu Y, Kirkman LA, Wellems TE (1996) *Proc Natl Acad Sci USA* 93:1130–1134.
27. Garapin AC, Colbere-Garapin F, Cohen-Solal M, Horodniceanu F, Kourilsky P (1981) *Proc Natl Acad Sci USA* 94:815–819.
28. Diez Silva MA (2005) Ph.D thesis (Université Pierre et Marie Curie, Paris).
29. Fidock DA, Wellems TE (1997) *Proc Natl Acad Sci USA* 94:10931–10936.
30. Pasvol G, Wilson RJ, Smalley ME, Brown J (1978) *Ann Trop Med Parasitol* 72:87–88.
31. Lambros C, Vanderberg JP (1979) *J Parasitol* 65:418–420.
32. Li J, Dao M, Lim CT, Suresh S (2005) *Biophys J* 88:3707–3719.
33. Dao M, Li J, Suresh S (2006) *Mater Sci Eng C* 26:1232–1244.
34. Henon S, Lenormand G, Richert A, Gallet F (1999) *Biophys J* 76:1145–1151.